*Human Molecular Genetics, 2010, Vol. 19, No. 7* **1221–1229**
*doi:10.1093/hmg/ddp592*
*Advance Access published on January 6, 2010*

# Molecular control of the cytosolic aconitase/IRP1 switch by extramitochondrial frataxin

**Ivano Condò, Florence Malisan, Ilaria Guccini, Dario Serio, Alessandra Rufini and Roberto Testi***

Laboratory of Signal Transduction, Department of Experimental Medicine and Biochemical Sciences, University of Rome 'Tor Vergata', Rome, Italy

Received September 16, 2009; Revised December 4, 2009; Accepted December 31, 2009

**The inability to produce normal levels of the mitochondrial protein frataxin causes the hereditary degenerative disorder Friedreich's Ataxia (FRDA), a syndrome characterized by progressive gait instability, cardiomyopathy and high incidence of diabetes. Frataxin is an iron-binding protein involved in the biogenesis of iron–sulfur clusters (ISC), prosthetic groups allowing essential cellular functions such as oxidative phosphorylation, enzyme catalysis and gene regulation. Although several evidence suggest that frataxin acts as an iron-chaperone within the mitochondrial compartment, we have recently demonstrated the existence of a functional extramitochondrial pool of mature frataxin in various human cell types. Here, we show that a similar proteolytic process generates both mature mitochondrial and extramitochondrial frataxin. To address the physiological function of human extramitochondrial frataxin, we searched for ISC-dependent interaction partners. We demonstrate that the extramitochondrial form of frataxin directly interacts with cytosolic aconitase/iron regulatory protein-1 (IRP1), a bifunctional protein alternating between an enzymatic and a RNA-binding function through the 'iron–sulfur switch' mechanism. Importantly, we found that the cytosolic aconitase defect and consequent IRP1 activation occurring in FRDA cells are reversed by the action of extramitochondrial frataxin. These results provide new insight into the control of cytosolic aconitase/IRP1 switch and expand current knowledge about the molecular pathogenesis of FRDA.**

## INTRODUCTION

Frataxin is an iron-binding protein strictly conserved during evolution, from proteobacteria to humans (1). Although different evidence indicates an involvement of frataxin in intracellular iron homeostasis (2), the primary function of this protein is still elusive. Frataxin deficiency clearly leads to defective iron–sulfur clusters (ISC) and heme biosynthesis, with further consequences concerning mitochondrial iron overload, impaired mitochondrial respiration, low ATP production, oxidative damage and enhanced stress-induced apoptosis (3). The ISC-dependent proteins play an essential role in several aspects of cellular metabolism including respiratory electron transfer, enzyme catalysis and DNA repair (4,5). Studies in yeast models have shown that biogenesis of ISC requires a large number of proteins catalyzing the process (4). The central components are those involved in transient assembly of ISC on a scaffold protein, within mitochondria. Isu1/ISCU acts as scaffold protein in all eukaryotes (6). The cysteine desulfurase Nfs1/ISCS provides the sulfur moiety, together with the Isd11 protein (7,8). Although the source of iron to synthesize ISC is less well defined, several data support the notion that frataxin is the iron donor of the reaction (9,10). In yeast, ISC biosynthesis seems to occur exclusively in the mitochondria. This hypothesis implies that mitochondria are indispensable to build all cellular ISC proteins, leading to the proposal that the preformed ISC are transported outside mitochondria by the ISC export machinery and finally inserted in extramitochondrial targets by the cytosolic ISC assembly (CIA) machinery (4). Little is known about the extramitochondrial ISC biogenesis in mammalian cells. Homologues of the yeast proteins involved in export and cytosolic assembly exist and are functional in humans (11–13). Moreover, extramitochondrial isoforms of the central components ISCU (14), NFU (15) and ISCS (16) have been identified in human cells.

*To whom correspondence should be addressed at: Department of Experimental Medicine and Biochemical Sciences, University of Rome 'Tor Vergata', Via Montpellier 1, 00133 Rome, Italy. Tel: +39 0672596503; Fax: +39 0672596505; Email: roberto.testi@uniroma2.it

Thus, mammalian biogenesis of extramitochondrial ISC shows partial similarity with the yeast's model, but nevertheless the pathways may be specified by fundamental distinctions.

In humans, a paradigm for frataxin defect is the degenerative disorder Friedreich's ataxia (FRDA). FRDA is an autosomal recessive monogenic disease characterized by progressive gait instability, loss of coordination, hypertrophic cardiomyopathy and increased incidence of diabetes mellitus (17). In almost all of the patients (95–98%), this disorder is caused by the homozygous hyperexpansion of a GAA-triplet repeat within the first intron of the FXN gene (18), a condition that results in lowered expression of the encoded frataxin protein (19). Human frataxin is synthesized as a 23 kDa precursor protein, which needs N-terminal proteolytic processing within the mitochondria to be converted into the functional mature form (20). Although initially considered a protein exclusively confined to the mitochondrial matrix (19), we and others recently demonstrated the existence of an extramitochondrial pool of mature frataxin in different human cell types (21–23). Extramitochondrial frataxin is a functionally relevant protein, since its expression directly suppresses apoptosis in transformed cell lines and protects FRDA patients' lymphoblasts from stress-induced cell death (22). A growing body of evidence indicates that mitochondrial frataxin acts as an iron-chaperone by providing ferrous iron ($Fe^{2+}$) in a bioavailable form. *In vitro* and *in vivo* studies proved that frataxin interacts with several proteins involved in the biogenesis of ISC: the scaffold ISCU/Isu1 (9,24), the chaperone GRP75 (25) and the adaptor protein ISD11 (25). Moreover, mitochondrial frataxin physically binds the ISC-containing enzymes ferrochelatase (26), succinate dehydrogenase (27) and mitochondrial aconitase (28,29). The direct interaction with ISC-dependent proteins reveals an additional role for frataxin in modulating the activity of its partners, as demonstrated by the protection/reactivation of mitochondrial aconitase (28).

In this study, we provide evidence for a physiological role of extramitochondrial frataxin in the cytoplasmic compartment. We first characterized the amino terminus of extramitochondrial frataxin generated in human cells. Our results indicate that the extramitochondrial frataxin matches the mature mitochondrial frataxin. Moreover, using a co-immunoprecipitation approach, we found that extramitochondrial frataxin directly interacts with the ISC-dependent cytosolic aconitase/iron regulatory protein-1 (IRP1) bifunctional protein. Importantly, we demonstrate that the cytosolic aconitase defect and consequent IRP1 activation in FRDA patients' cells can be reverted by extramitochondrial frataxin. Our findings suggest a direct function of frataxin in the regulation of cytosolic aconitase/IRP1 activity.

## RESULTS

### Mitochondrial processing generates the extramitochondrial frataxin

We previously reported that expression in human cells of wild-type frataxin cDNA (frataxin$^{1-210}$, FXN$^{1-210}$), encoding the 210 aminoacid precursor protein, generated a mature product that not only localized within mitochondria but also in the cytoplasm (22). This subcellular distribution is independent of forced expression, because endogenous extramitochondrial

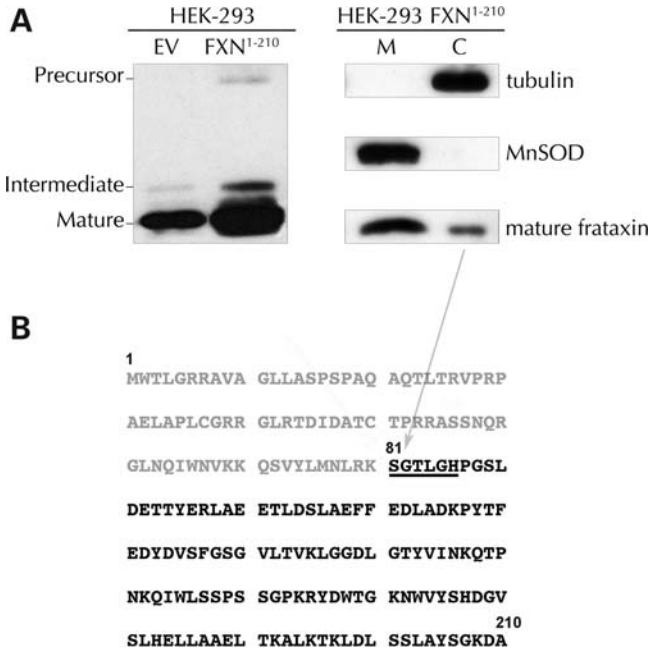


**Figure 1.** Mitochondrial processing generates the extramitochondrial frataxin. (**A**) Left panel: anti-frataxin western blot analysis of total extracts from HEK-293 cells stably transfected with either empty vector (EV) or wild-type frataxin$^{1-210}$ (FXN$^{1-210}$); precursor, intermediate and mature forms of frataxin are indicated. Right panel: western blot analysis of mitochondrial (M) and cytosolic (C) extracts from HEK-293 cells stably transfected with FXN$^{1-210}$. (**B**) Edman degradation analysis was performed on frataxin immunopurified from FXN$^{1-210}$ cytosolic extracts. The arrow shows the band that was sequenced and the position of obtained N-terminal residues (underlined) within the frataxin sequence.

frataxin is detectable in primary cells as well as in tumor cell lines (21–23). To better characterize extramitochondrial frataxin, we took advantage of the Flp-In-293 cells stably expressing FXN$^{1-210}$ previously described (20) (Fig. 1A, left panel). The stable expression of FXN$^{1-210}$ results mainly in accumulation of the mature mitochondrial product, generated by a proteolytic cleavage between Lys80 and Ser81 (FXN$^{81-210}$; 20). Furthermore, subcellular fractionations showed the presence of the extramitochondrial form in the cytosolic fractions prepared from the above cells (20). HEK-293 cells stably expressing FXN$^{1-210}$ were then used to identify the N-terminus of the extramitochondrial frataxin. To this end, highly purified cytosolic fractions were prepared and checked by western blot analysis. The mature frataxin recovered from mitochondrial fractions comigrates with the extramitochondrial form obtained from cytosolic fractions (Fig. 1A, right panel). To rule out cross-contamination of fractions, mitochondrial matrix MnSOD and cytosoplasmic tubulin were used as controls. The purity of subcellular fractions was further confirmed by the analysis of additional mitochondrial and cytosolic markers (Supplementary Material, Fig. S1). Frataxin was immunoprecipitated from the above cytosolic fractions, resolved on SDS–PAGE and subjected to sequential Edman degradation. As summarized in Figure 1B the N-terminal sequence obtained was S-G-T-L-G-H, corresponding to the same residues previously identified in the N-terminus of mature frataxin generated

upon mitochondrial processing. Together, these results indicate that the extramitochondrial protein is a $FXN^{81-210}$ polypeptide and that a similar proteolytic processing accounts for both mature mitochondrial and extramitochondrial frataxin.

### Extramitochondrial frataxin physically interacts with the cytosolic aconitase/IRP1 protein

To address the physiological function of extramitochondrial frataxin, we investigated its involvement in regulation of cytosolic ISC. To this purpose, we searched for interaction partners of extramitochondrial frataxin in human cells. Given the ability of mitochondrial frataxin to act as an iron-chaperone that interacts with mitochondrial aconitase by modulating its ISC-dependent enzyme activity, we reasoned that a corresponding interaction between their cytosolic counterparts could be possible. To determine if extramitochondrial frataxin and cytosolic aconitase/IRP1 share the same subcellular localization, HEK-293 cells were transiently transfected with extramitochondrial $FXN^{81-210}$ together with a Myc-tagged IRP1 (Myc-IRP1) and analyzed by immunofluorescence microscopy. As expected, both proteins were predominantly located in the cytoplasm. The merged images demonstrate their co-localization as revealed by the yellow areas (Fig. 2A). To test for the possible interaction between extramitochondrial frataxin and cytosolic aconitase/IRP1, we carried out a co-immunoprecipitation approach. HEK-293 cells were transiently transfected with either empty vector (EV), $FXN^{1-210}$ or extramitochondrial $FXN^{81-210}$ together with Myc-IRP1. In order to avoid artefactual interactions caused by excessive overexpression of Myc-IRP1, HEK-293 cells were transfected with amounts of the corresponding construct leading to moderated expression levels (Supplementary Material, Fig. S2). Cell extracts from transfected cells were immunoprecipitated with anti-frataxin mAb, and anti-Myc immunoblot analysis demonstrated the co-purification of Myc-IRP1 (Fig. 2B). Conversely, immunoprecipitation of Myc-IRP1 with anti-Myc resulted in co-purification of frataxin, as detected by anti-frataxin immunoblot analysis (Fig. 2C). In neither case negative control for immunoprecipitations with an irrelevant isotype-matching antibody or without antibody allowed detection of the above proteins (Fig. 2D). Notably, in both cases the interaction is evident in the absence of frataxin overexpression, demonstrating that endogenous extramitochondrial frataxin is sufficient to bind transfected Myc-IRP1. The interaction is slightly increased in $FXN^{1-210}$-transfected cells and it is strongly enhanced in the presence of transfected frataxin$^{81-210}$ ($FXN^{81-210}$). To further characterize the interaction, we examined if the binding between $FXN^{81-210}$ and cytosolic aconitase is modulated by the presence of enzyme's ISC. We generated a mutant protein (IRP1 C437S) lacking a critical cysteine responsible for coordination of the cluster. This mutant lacks aconitase activity and displays only the RNA-binding activity (30,31). As shown in Figure 3, immunoprecipitation and immunoblot analysis in both directions demonstrate that the presence of C437S substitution in IRP1 strongly inhibited the interaction with extramitochondrial frataxin.

These data collectively demonstrate that $FXN^{81-210}$ can directly interact with cytosolic aconitase/IRP1 in the extramitochondrial compartment.

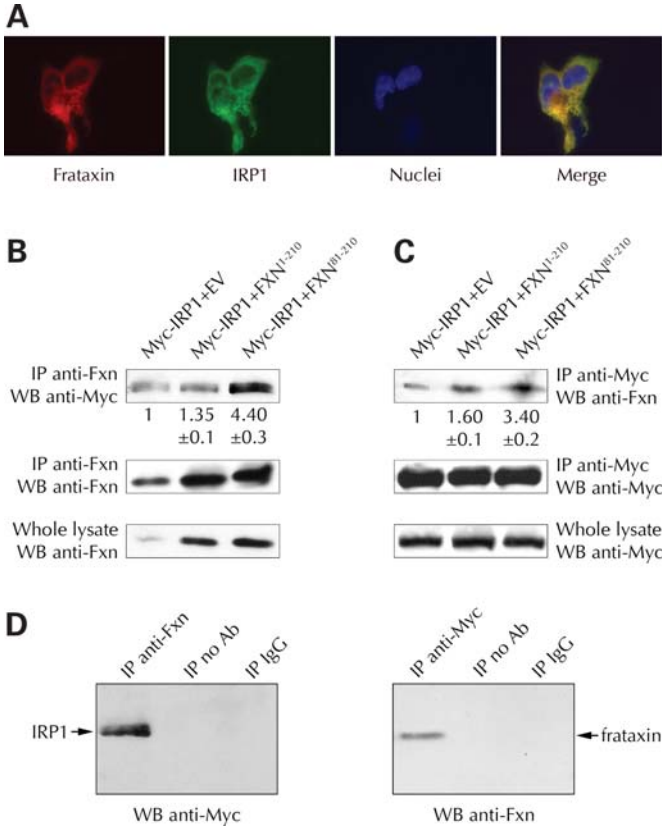


**Figure 2.** Extramitochondrial frataxin physically interacts with the cytosolic aconitase/IRP1 protein. (**A**) HEK-293 cells were transiently transfected with extramitochondrial frataxin$^{81-210}$ ($FXN^{81-210}$) together with a Myc-tagged IRP1 (Myc-IRP1) and analyzed by immunofluorescence with anti-frataxin (red), anti-IRP1 (green) and the nuclear DAPI stain (blue). The last panel shows the merged image. (**B**) HEK-293 cells were transiently transfected with either EV, $FXN^{1-210}$ or extramitochondrial $FXN^{81-210}$ together with a Myc-IRP1. Cell extracts were immunoprecipitated with anti-frataxin antibody and immunoblotted with anti-Myc antibody or anti-frataxin antibody. (**C**) HEK-293 cells were transiently transfected as in (B). Cell extracts were immunoprecipitated with anti-Myc antibody and immunoblotted with anti-frataxin antibody or anti-Myc antibody. The results are representative of three independent experiments. The densitometric quantitation of frataxin or IRP1 co-immunoprecipitated in the various samples is indicated (mean $\pm$ 1 SD). (**D**) HEK-293 cells were transiently transfected with $FXN^{81-210}$ together with Myc-IRP1. Left panel: cell extracts were immunoprecipitated with anti-frataxin antibody (IP anti-Fxn), without antibody (IP no Ab) or with an irrelevant isotype-matching antibody (IP IgG) and immunoblotted with anti-Myc antibody. Right panel: cell extracts were immunoprecipitated with anti-Myc antibody (IP anti-Myc), without antibody (IP no Ab) or with an irrelevant isotype-matching antibody (IP IgG) and immunoblotted with anti-frataxin antibody.

### Extramitochondrial frataxin rescues the cytosolic aconitase activity

As known, reduced frataxin expression determines a contemporary loss in activity of mitochondrial and cytosolic aconitases (32,33), two ISC-requiring enzymes encoded by two different genes (34). To investigate the functional implications of the interaction between extramitochondrial frataxin and cytosolic aconitase/IRP1, we looked for a functional relationship between frataxin localization and aconitase activity. To this purpose, frataxin-deficient lymphoblasts derived from a FRDA patient were stably reconstituted with either an EV,

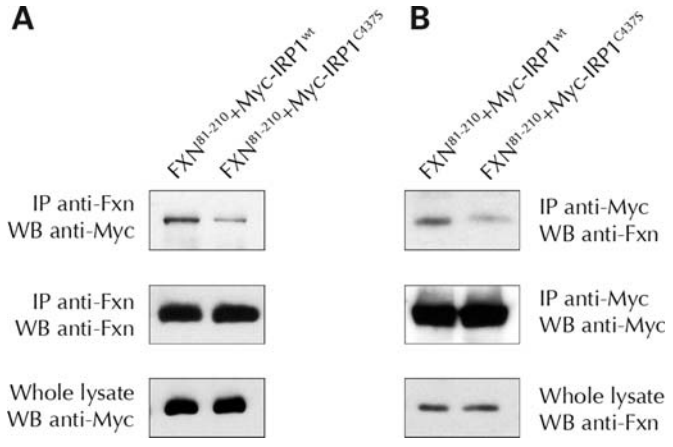


**Figure 3.** ISC-dependent interaction between extramitochondrial frataxin and cytosolic aconitase/IRP1. HEK-293 cells were transiently transfected with either wild-type (wt) or mutated (C437S) Myc-IRP1 together with extramitochondrial $FXN^{81-210}$. (**A**) Cell extracts were immunoprecipitated with anti-frataxin antibody and immunoblotted with anti-Myc antibody or anti-frataxin antibody. (**B**) Cell extracts were immunoprecipitated with anti-Myc antibody and immunoblotted with anti-frataxin antibody or anti-Myc antibody. The results are representative of three independent experiments.

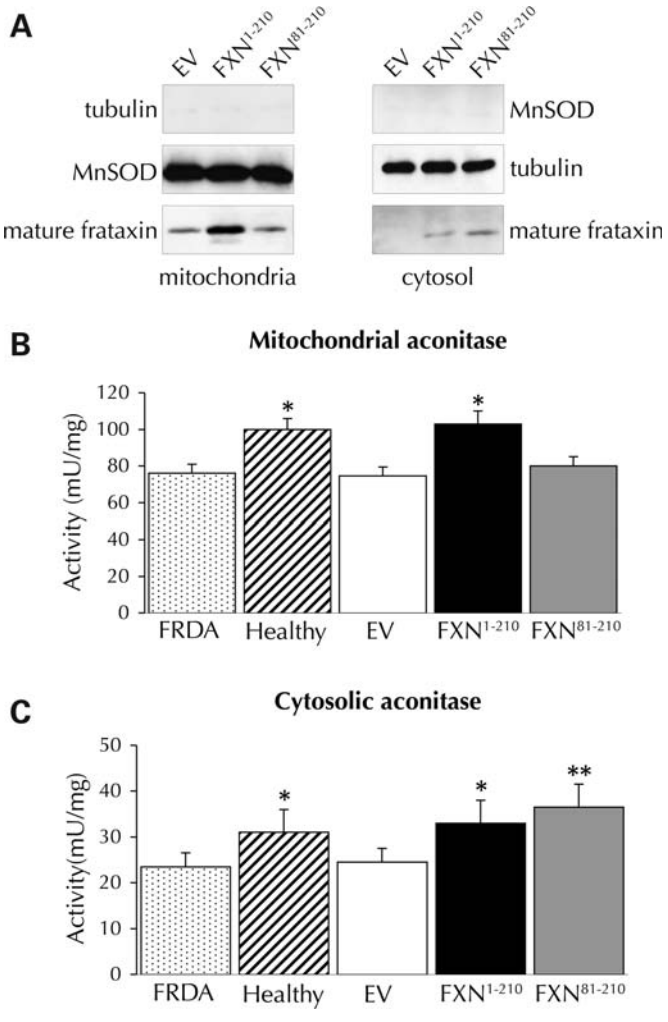


**Figure 4.** Extramichondrial frataxin rescues the cytosolic aconitase defect. (**A**) Western blot analysis of mitochondrial and cytosolic extracts from FRDA cells stably transfected with either EV, $FXN^{1-210}$ or extramitochondrial $FXN^{81-210}$. Aconitase assays were performed with mitochondrial (**B**) or cytosolic extracts (**C**) from lymphoblasts derived from a FRDA patient (FRDA), from his healthy brother (Healthy) and from the patient lymphoblasts stably reconstituted with either EV, $FXN^{1-210}$ or extramitochondrial $FXN^{81-210}$. Error bars in the graph indicate 1 SD. Statistical analysis by Student's *t*-test: $^{*}P < 0.05$; $^{**}P < 0.01$.

$FXN^{1-210}$ or extramitochondrial $FXN^{81-210}$ (Fig. 4A) and total and subcellular protein extracts were assayed for aconitase activity. To evaluate the status of both aconitases, two independent activity assays were used. Enzyme activity was monitored both in subcellular fractions, by spectrophotometric analysis (Fig. 4B and C), and in total lysates, by native in-gel assays (Fig. 5). As expected, both mitochondrial and cytosolic extracts from FRDA lymphoblasts show a significant deficit of aconitase activity with respect to control lymphoblasts derived from an healthy brother of the patient (Figs 4 and 5). Mitochondrial aconitase is rescued in FRDA cells reconstituted with $FXN^{1-210}$ but could not be significantly restored in FRDA cells reconstituted with $FXN^{81-210}$ (Figs 4B and 5B). On the other hand, although cytosolic aconitase is rescued in FRDA cells reconstituted with $FXN^{1-210}$, it is even more efficiently rescued in FRDA cells reconstituted with $FXN^{81-210}$. The in-gel assay fully confirmed this finding (Fig. 5). Furthermore, since the native in-gel assay allows the simultaneous visualization of both activities, we could quantitate the relative contribution of the cytosolic enzyme with respect to the total aconitase activity. We calculated that the cytosolic aconitase represents ~16% of total cellular aconitase activity in EV-reconstituted FRDA lymphoblasts. The simultaneous effect on the activity of both isozymes did not significantly change this proportion in $FXN^{1-210}$-reconstituted FRDA cells, whereas the reconstitution with $FXN^{81-210}$ raised the percent of the cytosolic activity to ~30% of total, mostly due to a specific boost of the cytosolic enzyme (Fig. 5B). These results suggest that extramitochondrial frataxin can directly affect the enzymatic activity of cytosolic aconitase.

### Extramitochondrial frataxin modulates the RNA-binding activity of IRP1

The enzymatic activity of cytosolic aconitase and the RNA-binding activity of IRP1 are two mutually exclusive functions of the same protein. The presence of a 4Fe–4S cluster allows its enzymatic function as aconitase, whereas a complete loss of this cofactor triggers its mRNA-binding ability (35). We thus analyzed FRDA lymphoblasts for the iron responsive element (IRE)-binding ability of IRP1. As previously reported for FRDA patient cells (36,37), as well as for a human cell model of frataxin depletion (33), we found that FRDA lymphoblasts showed increased IRP1 activity compared with their healthy control (Fig. 6A). RNA band-shift analysis indicates a strong increase of IRPs-binding activity without any variation of IRP1 expression levels between FRDA and control cells, as judged by *in vitro* β-mercaptoethanol activation and by western blot studies (Fig. 6A). In this band-shift assay human IRP1 and IRP2 comigrate. IRP2 is another IRE-binding protein which is not an ISC-dependent protein and

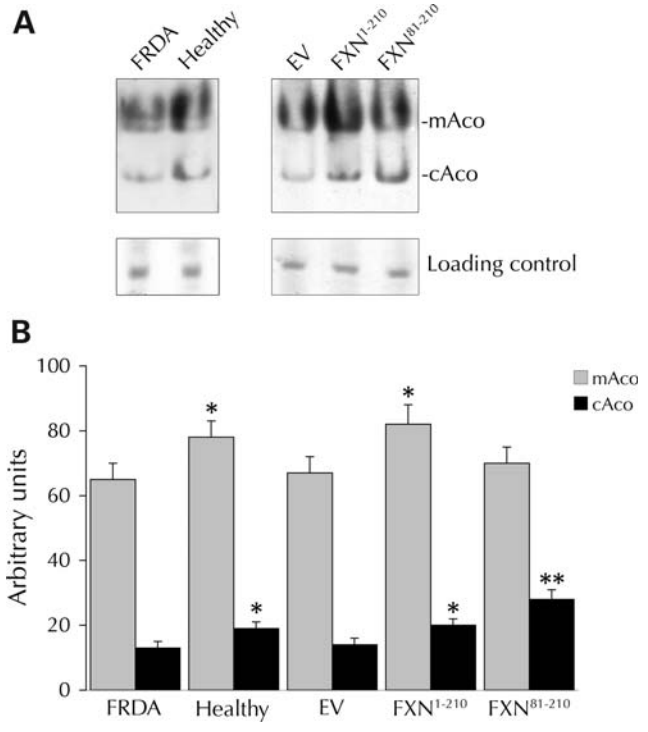


**Figure 5.** Extramichondrial frataxin specifically boosts cytosolic aconitase. (**A**) Aconitase in-gel assays were performed with total extracts from patient lymphoblasts (FRDA), from control lymphoblasts (Healthy) and from the patient lymphoblasts stably reconstituted with either EV, $FXN^{1-210}$ or extramitochondrial $FXN^{81-210}$; the bands corresponding to mitochondrial aconitase (mAco) and cytosolic aconitase (cAco) are indicated. Loading control represents an irrelevant coomassie-stained band from the above gel. The results are representative of four independent experiments. (**B**) The mitochondrial (grey bar) and cytosolic (black bar) aconitase activities were calculated by densitometric analysis of four independent native in-gel assays. Error bars in the graph indicate 1 SD. Statistical analysis by Student's *t*-test: $^{*}P < 0.05$; $^{**}P < 0.01$.

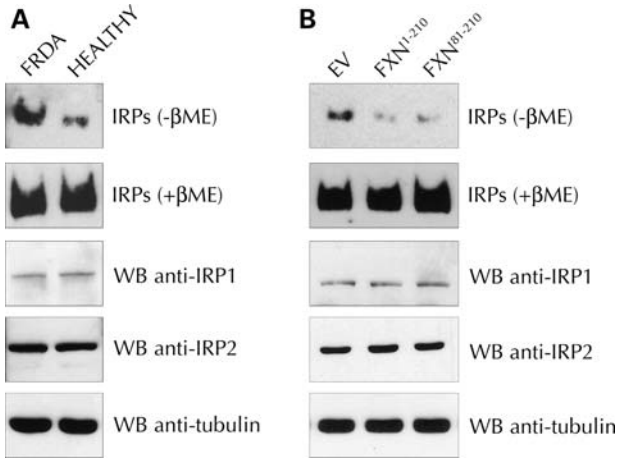


**Figure 6.** Extramitochondrial frataxin inhibits IRP1 RNA-binding activity. (**A**) Cell extracts from a FRDA patient (FRDA) and from healthy control lymphoblasts (Healthy) were incubated with an IRE RNA probe, with or without 3% β-mercaptoethanol (βME) which fully activates IRP1-binding ability, and analyzed for IRPs band shift by 6% native PAGE. The same extracts were analyzed for IRP1 and IRP2 expression levels by western blotting. (**B**) Cell extracts from the patient lymphoblasts stably reconstituted with either EV, $FXN^{1-210}$ or extramitochondrial $FXN^{81-210}$ were analyzed for IRPs band shift and IRPs protein levels as in (A).

whose activity is regulated through protein degradation. To exclude a contribution of IRP2, protein expression level was therefore analyzed in control and FRDA cells. Western blot analysis revealed equal levels of IRP2, thus confirming an exclusive activation of IRP1-binding activity in the above FRDA lymphoblasts (Fig. 6A). We then performed experiments to examine the effects of extramitochondrial frataxin on IRP1 activation. Extracts from FRDA cells stably reconstituted with either EV, $FXN^{1-210}$ or $FXN^{81-210}$ were analyzed by RNA band-shift and western blotting (Fig. 6B). RNA band-shift showed a marked reduction of IRPs-binding activity in $FXN^{1-210}$-reconstituted FRDA cells compared with corresponding EV-reconstituted FRDA cells (Fig. 6B). This effect is indistinguishable from that observed in $FXN^{81-210}$-reconstituted FRDA cells (Fig. 6B), demonstrating the specific action of extramitochondrial frataxin on IRP1 status. The reduced IRPs activity cannot be accounted by altered IRP1 expression levels, as judged by *in vitro* β-mercaptoethanol activation and by western blot studies (Fig. 6B), consistent with the fact that extramitochondrial frataxin functionally converts IRP1 to its cytosolic aconitase form. Moreover, western blots confirmed that IRP2 protein levels were not altered (Fig. 6B), ruling out a contribution by IRP2. Collectively, the data indicate that the extramitochondrial form of human frataxin plays a critical function in the cytosolic aconitase/IRP1 switch.

## DISCUSSION

In the past few years, the understanding of the function of frataxin has grown rapidly (3). Consequently, pathophysiological defects of FRDA have become more comprehensible, thus allowing the design of new therapeutic approaches (38–40). However, the molecular function of this protein was investigated mainly with respect to mitochondrial physiology. Subcellular localization of frataxin in mammalian cells is currently under debate. Recently, an extramitochondrial pool of mature frataxin was detected in several cell types of human origin (21–23). We demonstrated that overexpression of extramitochondrial frataxin confers protection against stress-induced apoptosis in frataxin-deficient cells (22). Moreover, forced expression of wild-type frataxin precursor in different cell lines leads to a substantial production of a frataxin form that does not reside in the mitochondrial compartment (20,22). Strikingly, in the microsporidian parasite *Trichomonas hominis*, which has mitosomes instead of mitochondria, the main pool of frataxin is located in the cytosol (41). In contrast to the mitochondrial frataxin, very little is known about biogenesis and function of extramitochondrial frataxin. A recent analysis of the mitochondrial maturation process allowed us to identify for the first time the 14 kDa active form of mature frataxin generated in human living cells (20). In the present study, we have made an effort to characterize the mature extramitochondrial form. Edman degradation of extramitochondrial frataxin purified from living cells indicates that this form has an amino terminus starting with Ser81. The N-terminal sequence obtained corresponds to that previously identified in the N-terminus of

mature frataxin generated upon mitochondrial processing (20). These results demonstrate that both mitochondrial and extramitochondrial isoforms are identical $FXN^{81-210}$ polypeptides. Thus, our data support a view in which mature $FXN^{81-210}$ is first produced by a two-step mitochondrial proteolytic process and then it is partially exported outside the mitochondria by a still unknown mechanism. The multiple distribution of a protein between subcellular compartments usually arises from multiple transcription start sites, alternative splicing or different translation initiations (42). On the contrary, the notion that mature mitochondrial and extramitochondrial frataxin are identical is reminiscent of the dual targeting of yeast fumarase enzyme (43). Similarly to frataxin, the fumarase precursor is directed to mitochondria and matured by mitochondrial processing peptidase. A subset of mature fumarase is then imported into the matrix, whereas another part is released in the cytosol by retrograde movement through the translocation pore (44). As a result of such mechanism, mitochondrial and cytosolic forms of yeast fumarase share identical N-termini (45).

To investigate the metabolic role of extramitochondrial frataxin, we sought to identify its cytosolic targets. Mitochondrial frataxin is a double-side modulator of mitochondrial aconitase activity. First, the role of frataxin in the biosynthesis of ISC impacts on cellular availability of prosthetic group required for enzyme's function (32,33). Second, frataxin directly chaperones $Fe^{2+}$ to the inactive 3Fe–4S cluster of mitochondrial aconitase in order to reconstitute a functional 4Fe–4S cluster (28). Two distinct genes encode mammalian mitochondrial and cytosolic aconitases. Both proteins require a 4Fe–4S cluster for enzymatic activity. Moreover, the two aconitases share 30% overall identity, showing a striking overlap of active site residues (46). By co-expression in HEK-293 cells, we demonstrate that extramitochondrial frataxin co-localizes and interacts with cytosolic aconitase/IRP1 protein. Immunoprecipitation of transfected frataxin results in co-precipitation of transfected IRP1, and this is confirmed by the reverse approach. Strikingly, physical association between the two proteins is evident without a forced expression of extramitochondrial frataxin. This provides additional evidence that human cells express a functional endogenous frataxin in the cytoplasm. Moreover, we report that such interaction is largely, although not exclusively, dependent on the presence of an ISC inserted into the cytosolic aconitase form. Through the so-called 'ISC-switch' cytosolic aconitase/IRP1 alternates between two mutually exclusive functions: the ISC-containing form is an enzyme converting cytosolic citrate to isocitrate, whereas the ISC-devoid form regulates gene expression by the binding to specific mRNA targets (35). The defective activity of mitochondrial and cytosolic aconitases, as well as an increased IRP1 RNA-binding activity, are clearly associated with frataxin deficiency in model organisms (47–49), in human cell cultures (23,33) and in patients affected by FRDA (32,36,37). We looked for a compartment-specific function of frataxin on aconitases activity. Our results indicate that expression of $FXN^{1-210}$ in FRDA cells rescues the activity of both mitochondrial and cytosolic aconitases. Moreover, IRP1 activity returns to basal levels. Conversely, expression of $FXN^{81-210}$ impacts on IRP1-binding ability and activates the cytosolic aconitase, without an evident effect on the mitochondrial one. Given that FRDA cells show a localization of frataxin in both compartments when reconstituted with $FXN^{1-210}$ (Fig. 3A), the above data strongly suggest a compartment-specific role for frataxin forms. Accordingly, cytosolic aconitase activity was described to decline in parallel with cytosolic frataxin depletion, with no significant deficit in mitochondrial aconitase activity, until depletion of the mitochondrial frataxin pool (23).

In view of the physical interaction between extramitochondrial frataxin and cytosolic aconitase/IRP1, protection or reactivation of enzyme's ISC represents a major hypothesis for the cytosolic function of frataxin. The molecular mechanisms by which cytosolic aconitase is converted to its IRE binding form are still enigmatic. The 4Fe–4S cluster of cytosolic aconitase is highly sensitive to reactive oxygen species and reactive nitrogen species (50). These perturbants lead to loss of the labile $Fe_\alpha$ atom by generating a transient 3Fe–4S cluster (51–53), followed by a complete removal of covalent linkages between aconitase and its cofactor (54). The protein containing a 3Fe–4S cluster was reported to possess neither enzyme activity nor RNA binding activity; however, it can be reverted to the aconitase form by $Fe^{2+}$ supply (51). As recently demonstrated (55), the equilibrium of cycling between 4Fe–4S and 3Fe–4S seems critical for conversion to the RNA binding form. Because oxidative stress endogenously occurs in FRDA cells, cytosolic aconitase deficit and IRP1 activation are ascribed, at least in part, to an excessive ISC damage. Thus, although not directly addressed by this work, extramitochondrial frataxin could impact on the 3Fe–4Fe equilibrium by direct delivery of $Fe^{2+}$ to damaged 3Fe–4S cluster of cytosolic aconitase. Moreover, a more general role in biogenesis of cytosolic ISC cannot be excluded and will require further investigations. In this regard, extramitochondrial frataxin was described to interact with the cytosolic isoform of ISCU (cISCU or ISCU1) (21), a scaffold protein for ISC biosynthesis. The isoform specific depletion of human mitochondrial and cytosolic ISCU provided evidence for a selective function in their respective compartments (14). Although silencing of cISCU resulted in only slight changes in the steady-state activity of cytosolic aconitase, the impact on ISC repair/regeneration toward this enzyme is strongly evident (14). In addition, two recently identified homologues of the yeast CIA machinery were involved in maturation of cytosolic ISC in mammals. As a result, RNAi knockdown of IOP1 (12; homologue of yeast Nar1) or huNbp35/Nubp1 (13; homologue of yeast Nbp35) impairs activity of cytosolic aconitase and activates IRP1-binding ability, whereas mitochondrial aconitase remains intact.

Results presented here provide the first evidence on the molecular control of cytosolic aconitase/IRP1 activity by extramitochondrial frataxin. These data propose an extramitochondrial role for frataxin in the emerging pathways governing cytosolic ISC-dependent proteins in humans and contribute to a better understanding of molecular pathophysiology of FRDA.

## MATERIALS AND METHODS

### cDNA expression constructs and cell transfections

The pIRES2/$FXN^{1-210}$, pIRES2/$FXN^{81-210}$ and pcDNA3/$FXN^{81-210}$ constructs were described elsewhere (20). Human

IRP1 cDNA containing *Xho*I site at 5′-end/*Xba*I at 3′-end was obtained by PCR from the clone MGC-8709 (ATCC) and inserted in pcDNA3Myc vector to express an N-terminal Myc-IRP1 protein. The mutant construct pcDNA3Myc/IRP1$^{C437S}$ was generated using the QuickChange site-directed mutagenesis kit (Stratagene) using pcDNA3Myc/IRP1 as template. All final constructs were verified by sequencing. GM15850B lymphoblasts, from a clinically affected FRDA patient and GM15851B lymphoblasts from a clinically unaffected brother of GM15850 were obtained from NIGMS Human Genetic Cell Repository, Coriell Institute for Medical Research. FRDA lymphoblasts were stably transfected by electroporation and selected with 500 μg/ml G418 (Invitrogen) as reported (20). Human embryonic kidney HEK-293 cells were transiently transfected with 20 μg total DNA using Lipofectamine 2000 (Invitrogen) following the manufacturer's instructions.

### Subcellular fractionations

Mitochondrial and cytosolic extracts were prepared as previously described (22) with minor modifications. Cells were harvested, washed twice with ice-cold PBS and resuspendend into an ice-cold isotonic buffer (210 mM mannitol, 70 mM sucrose, 10 mM HEPES pH 7.4, 1 mM EDTA and 1 mM DTT) supplemented with Complete protease inhibitor cocktail (Roche). The suspension was left on ice and mixed periodically for 20 min, then passed through a 25-gauge syringe needle several times. The homogenate was centrifuged twice at 800*g* for 10 min at 4°C to eliminate nuclei and unbroken cells. The supernatant was further centrifuged twice at 10 000*g* for 30 min at 4°C and collected as the cytosolic fraction. The mitochondrial pellet was resuspended in the above isotonic buffer containing 0.5% Triton X-100 and Complete cocktail. After a 20 min incubation on ice, the sample was centrifuged at 14 000*g* for 15 min at 4°C and the resulting supernatant was collected as the mitochondrial fraction.

### Purification and N-terminal sequencing of extramitochondrial frataxin

Frataxin was immunoprecipitated from ∼50 mg of cytosolic extracts from Flp-In-293 cells stably expressing FXN$^{1-210}$ (20) with mAb anti-frataxin (MAB-10876 Immunological Sciences) and protein G-sepharose beads (GE Healthcare Life Sciences). Immunocomplexes were then resolved by 15% SDS–PAGE and coomassie-stained bands were excised from the gel. N-terminal aminoacid sequence was determined by automated Edman degradation performed by Alta Bioscience (University of Birmingham, UK).

### Immunofluorescence analysis

HEK-293 cells were plated onto glass chamber slides (Lab-Tek) and grown in complete medium for an additional day after plating. Cells were then co-transfected with pcDNA3/FXN$^{81-210}$ and pcDNA3/Myc-IRP1 (1:1) using Lipofectamine 2000 (Invitrogen) following the manufacturer's instructions. Twenty-four hours after transfection, cells were fixed for 15 min with 4% paraformaldehyde in phosphate-buffered saline (PBS) at room temperature (RT). Coverslips were rinsed twice with PBS and permeabilized for 30 min at 37°C with 60 μM digitonin, washed twice with PBS and followed by a blocking step, with PBS containing 10% FBS 1 h at RT to minimize non-specific staining. Samples were then incubated for 1 h at 37°C with anti-frataxin monoclonal antibody MAB-10876 or isotype-matched control mAb, diluted 1:400 in PBS/10% FBS. After three washing with PBS, cells were incubated for 1 h at RT with secondary Alexa 594-conjugated goat anti-mouse antibody (Molecular Probes) diluted 1:1000 in PBS/10% FBS, rinsed three times in PBS and then incubated with primary anti-IRP1 polyclonal rabbit antibody (a kind gift from Dr Sonia Levi, Vita-Salute San Raffaele University, Italy) diluted 1:200 in PBS/10% FBS. After three washing with PBS, cells were incubated for 1 h at RT with secondary Alexa 488-conjugated goat anti-rabbit antibody (Molecular Probes) diluted 1:1000 in PBS/10% FBS, rinsed three times in PBS and mounted on glass slides with Prolong Antifade (Molecular Probes). All images were acquired by using a BX60 Olympus microscope equipped with a Cohu High-performance CDD camera.

### Immunoprecipitation and western blotting

Cell extracts from HEK-293 cells transiently co-transfected with frataxin and Myc-IRP1 constructs were used to immunoprecipitate either frataxin by mAb anti-frataxin MAB-10876, or Myc-IRP1 by mAb anti-human c-myc 9E10 (554205 BD Pharmingen). Immunoprecipitates were separated by 12% SDS–PAGE, transferred on Protran nitrocellulose membranes (Whatman) and analyzed by immunoblotting using ECL system detection (GE Healthcare Life Sciences). To analyze total protein extracts, cells were lysed in ice-cold RIPA buffer supplemented with Complete protease inhibitor cocktail. Cell extracts were separated by 12 or 15% SDS–PAGE and immunoblotted with the following antibodies: mAb anti-frataxin (MAB-10876 Immunological Sciences), mAb anti-α-Tubulin (Sigma), anti-MnSOD (StressGen), mAb anti-c-myc 9E10 (BD Pharmingen), anti-IRP1 N-17 (sc-14216 Santa Cruz Biotechnology) and mAb anti-IRP2 7H6 (sc-33682 Santa Cruz Biotechnology).

### Aconitase assays

Aconitase activity was measured spectrophotometrically at 340 nm by a coupled reaction of aconitase and isocitrate dehydrogenase. The assay reactions contained 50–100 μg of subcellular fractions in 50 mM Hepes pH 7.4, 1 mM sodium citrate, 0.6 mM $MnCl_2$, 0.2 mM $NADP^+$ and 2 U/ml isocitrate dehydrogenase from porcine heart (Sigma-Aldrich). For the calculation of the activities, 1 milliunit of enzyme was defined as the amount of protein that converted 1 nmol of $NADP^+$ in 1 min at 25°C.

The aconitase in-gel assay was performed as described (14). Briefly, 100 μg of total extracts from cells lysed in CelLytic M buffer (Sigma-Aldrich) with Complete cocktail were resolved in a 4% stacking, 8% separating gel by electrophoretic run at 18 V/cm for 3.5 h at 4°C. Densitometric quantitation was obtained using ImageJ software.

Statistical analysis was performed using a Student's *t*-test; all values are expressed as means ± SD.

### IRPs RNA band-shift (RNA EMSA)

The probe used was a 32-mer RNA oligonucleotide corresponding to IRE sequence from human H-ferritin gene (5′-GGU UUC CUG CUU CAA CAG UGC UUG GAC GGA AC-3′), labeled with a biotin molecule at 5′ end (Metabion International AG). Cell lysates were prepared in CelLytic M buffer supplemented with Complete cocktail. Binding reaction contained 5–10 μg of total extracts in a final volume of 15–20 μl containing 10 mM Hepes pH 7.4, 40 mM KCl, 3 mM $MgCl_2$ and 5% glycerol. When needed, β-mercaptoethanol was included to a final concentration of 3% in order to fully activate IRP1-binding ability. After incubation at RT for 10 min, RNAse T1 (Sigma-Aldrich) was added for 10 min, followed by addition of 5 mg/ml heparin (Sigma-Aldrich) for another 10 min, both at RT. Binding reactions were separated by a 6% native PAGE in TBE 0.3X at 16 V/cm for 2 h at RT, transferred on Biodyne B Nylon Membranes (Pierce) and detected using Chemiluminescent Nucleic Acid Detection Module (Pierce).

## SUPPLEMENTARY MATERIAL

Supplementary Material is available at *HMG* online.

## ACKNOWLEDGEMENTS

We thank all colleagues in our laboratory for helpful discussion and Dr Natascia Ventura for critical reading of the manuscript. We also thank: Dr. Gaetano Cairo for helpful discussion in the development of IRP band-shift assay, Drs Alessandro Campanella and Sonia Levi for the anti-IRP1 rabbit serum.

*Conflict of Interest statement*. None declared.

## FUNDING

This work has been supported by National Ataxia Foundation, Ataxia UK and Friedreich's Ataxia Research Alliance. The financial support of Telethon-Italy (Grant GGP06059) is gratefully acknowledged. A.R. is a fellowship holder of the Fondazione Santa Lucia, Rome; I.G. is a fellowship holder of the Association Française de l'Ataxie de Friedreich (AFAF).

## REFERENCES

1. Bencze, K.Z., Kondapalli, K.C., Cook, J.D., McMahon, S., Millan-Pacheco, C., Pastor, N. and Stemmler, T.L. (2006) The structure and function of frataxin. *Crit. Rev. Biochem. Mol. Biol.*, **41**, 269–291.
2. Wilson, R.B. (2006) Iron dysregulation in Friedreich ataxia. *Semin. Pediatr. Neurol.*, **13**, 166–175.
3. Pandolfo, M. and Pastore, A. (2009) The pathogenesis of Friedreich ataxia and the structure and function of frataxin. *J. Neurol.*, **256** (Suppl. 1), 9–17.
4. Lill, R. and Muhlenhoff, U. (2008) Maturation of iron–sulfur proteins in eukaryotes: mechanisms, connected processes, and diseases. *Annu. Rev. Biochem.*, **77**, 669–700.
5. Rouault, T.A. and Tong, W.H. (2008) Iron–sulfur cluster biogenesis and human disease. *Trends Genet.*, **24**, 398–407.
6. Wu, G., Mansy, S.S., Wu Sp, S.P., Surerus, K.K., Foster, M.W. and Cowan, J.A. (2002) Characterization of an iron–sulfur cluster assembly protein (ISU1) from Schizosaccharomyces pombe. *Biochemistry*, **41**, 5024–5032.
7. Adam, A.C., Bornhovd, C., Prokisch, H., Neupert, W. and Hell, K. (2006) The Nfs1 interacting protein Isd11 has an essential role in Fe/S cluster biogenesis in mitochondria. *Embo J.*, **25**, 174–183.
8. Wiedemann, N., Urzica, E., Guiard, B., Muller, H., Lohaus, C., Meyer, H.E., Ryan, M.T., Meisinger, C., Muhlenhoff, U., Lill, R. *et al.* (2006) Essential role of Isd11 in mitochondrial iron–sulfur cluster synthesis on Isu scaffold proteins. *Embo J.*, **25**, 184–195.
9. Yoon, T. and Cowan, J.A. (2003) Iron–sulfur cluster biosynthesis. Characterization of frataxin as an iron donor for assembly of [2Fe–2S] clusters in ISU-type proteins. *J. Am. Chem. Soc.*, **125**, 6078–6084.
10. Foury, F., Pastore, A. and Trincal, M. (2007) Acidic residues of yeast frataxin have an essential role in Fe–S cluster assembly. *EMBO Rep.*, **8**, 194–199.
11. Cavadini, P., Biasiotto, G., Poli, M., Levi, S., Verardi, R., Zanella, I., Derosas, M., Ingrassia, R., Corrado, M. and Arosio, P. (2007) RNA silencing of the mitochondrial ABCB7 transporter in HeLa cells causes an iron-deficient phenotype with mitochondrial iron overload. *Blood*, **109**, 3552–3559.
12. Song, D. and Lee, F.S. (2008) A role for IOP1 in mammalian cytosolic iron–sulfur protein biogenesis. *J. Biol. Chem.*, **283**, 9231–9238.
13. Stehling, O., Netz, D.J., Niggemeyer, B., Rosser, R., Eisenstein, R.S., Puccio, H., Pierik, A.J. and Lill, R. (2008) Human Nbp35 is essential for both cytosolic iron–sulfur protein assembly and iron homeostasis. *Mol. Cell. Biol.*, **28**, 5517–5528.
14. Tong, W.H. and Rouault, T.A. (2006) Functions of mitochondrial ISCU and cytosolic ISCU in mammalian iron–sulfur cluster biogenesis and iron homeostasis. *Cell Metab.*, **3**, 199–210.
15. Tong, W.H., Jameson, G.N., Huynh, B.H. and Rouault, T.A. (2003) Subcellular compartmentalization of human Nfu, an iron–sulfur cluster scaffold protein, and its ability to assemble a [4Fe–4S] cluster. *Proc. Natl. Acad. Sci. USA*, **100**, 9762–9767.
16. Li, K., Tong, W.H., Hughes, R.M. and Rouault, T.A. (2006) Roles of the mammalian cytosolic cysteine desulfurase, ISCS, and scaffold protein, ISCU, in iron–sulfur cluster assembly. *J. Biol. Chem.*, **281**, 12344–12351.
17. Pandolfo, M. (2008) Friedreich ataxia. *Arch. Neurol.*, **65**, 1296–1303.
18. Campuzano, V., Montermini, L., Molto, M.D., Pianese, L., Cossee, M., Cavalcanti, F., Monros, E., Rodius, F., Duclos, F., Monticelli, A. *et al.* (1996) Friedreich's ataxia: autosomal recessive disease caused by an intronic GAA triplet repeat expansion. *Science*, **271**, 1423–1427.
19. Campuzano, V., Montermini, L., Lutz, Y., Cova, L., Hindelang, C., Jiralerspong, S., Trottier, Y., Kish, S.J., Faucheux, B., Trouillas, P. *et al.* (1997) Frataxin is reduced in Friedreich ataxia patients and is associated with mitochondrial membranes. *Hum. Mol. Genet.*, **6**, 1771–1780.
20. Condò, I., Ventura, N., Malisan, F., Rufini, A., Tomassini, B. and Testi, R. (2007) *In vivo* maturation of human frataxin. *Hum. Mol. Genet.*, **16**, 1534–1540.
21. Acquaviva, F., De Biase, I., Nezi, L., Ruggiero, G., Tatangelo, F., Pisano, C., Monticelli, A., Garbi, C., Acquaviva, A.M. and Cocozza, S. (2005) Extra-mitochondrial localisation of frataxin and its association with IscU1 during enterocyte-like differentiation of the human colon adenocarcinoma cell line Caco-2. *J. Cell. Sci.*, **118**, 3917–3924.
22. Condò, I., Ventura, N., Malisan, F., Tomassini, B. and Testi, R. (2006) A pool of extramitochondrial frataxin that promotes cell survival. *J. Biol. Chem.*, **281**, 16750–16756.
23. Lu, C. and Cortopassi, G. (2007) Frataxin knockdown causes loss of cytoplasmic iron–sulfur cluster functions, redox alterations and induction of heme transcripts. *Arch. Biochem. Biophys.*, **457**, 111–122.
24. Gerber, J., Muhlenhoff, U. and Lill, R. (2003) An interaction between frataxin and Isu1/Nfs1 that is crucial for Fe/S cluster synthesis on Isu1. *EMBO Rep.*, **4**, 906–911.
25. Shan, Y., Napoli, E. and Cortopassi, G. (2007) Mitochondrial frataxin interacts with ISD11 of the NFS1/ISCU complex and multiple mitochondrial chaperones. *Hum. Mol. Genet.*, **16**, 929–941.
26. Yoon, T. and Cowan, J.A. (2004) Frataxin-mediated iron delivery to ferrochelatase in the final step of heme biosynthesis. *J. Biol. Chem.*, **279**, 25943–25946.
27. Gonzalez-Cabo, P., Vazquez-Manrique, R.P., Garcia-Gimeno, M.A., Sanz, P. and Palau, F. (2005) Frataxin interacts functionally with

mitochondrial electron transport chain proteins. *Hum. Mol. Genet.*, **14**, 2091–2098.
28. Bulteau, A.L., O'Neill, H.A., Kennedy, M.C., Ikeda-Saito, M., Isaya, G. and Szweda, L.I. (2004) Frataxin acts as an iron chaperone protein to modulate mitochondrial aconitase activity. *Science*, **305**, 242–245.
29. Bulteau, A.L., Lundberg, K.C., Ikeda-Saito, M., Isaya, G. and Szweda, L.I. (2005) Reversible redox-dependent modulation of mitochondrial aconitase and proteolytic activity during *in vivo* cardiac ischemia/reperfusion. *Proc. Natl. Acad. Sci. USA*, **102**, 5987–5991.
30. Hirling, H., Henderson, B.R. and Kuhn, L.C. (1994) Mutational analysis of the [4Fe–4S]-cluster converting iron regulatory factor from its RNA-binding form to cytoplasmic aconitase. *EMBO J.*, **13**, 453–461.
31. Wang, J., Fillebeen, C., Chen, G., Biederbick, A., Lill, R. and Pantopoulos, K. (2007) Iron-dependent degradation of apo-IRP1 by the ubiquitin-proteasome pathway. *Mol. Cell. Biol.*, **27**, 2423–2430.
32. Rotig, A., de Lonlay, P., Chretien, D., Foury, F., Koenig, M., Sidi, D., Munnich, A. and Rustin, P. (1997) Aconitase and mitochondrial iron–sulphur protein deficiency in Friedreich ataxia. *Nat. Genet.*, **17**, 215–217.
33. Stehling, O., Elsasser, H.P., Bruckel, B., Muhlenhoff, U. and Lill, R. (2004) Iron–sulfur protein maturation in human cells: evidence for a function of frataxin. *Hum. Mol. Genet.*, **13**, 3007–3015.
34. Tong, W.H. and Rouault, T.A. (2007) Metabolic regulation of citrate and iron by aconitases: role of iron–sulfur cluster biogenesis. *Biometals*, **20**, 549–564.
35. Rouault, T.A. (2006) The role of iron regulatory proteins in mammalian iron homeostasis and disease. *Nat. Chem. Biol.*, **2**, 406–414.
36. Lobmayr, L., Brooks, D.G. and Wilson, R.B. (2005) Increased IRP1 activity in Friedreich ataxia. *Gene*, **354**, 157–161.
37. Li, K., Besse, E.K., Ha, D., Kovtunovych, G. and Rouault, T.A. (2008) Iron-dependent regulation of frataxin expression: implications for treatment of Friedreich ataxia. *Hum. Mol. Genet.*, **17**, 2265–2273.
38. Cooper, J.M. and Schapira, A.H.V. (2007) Friedreich's ataxia: coenzyme Q10 and vitamin E therapy. *Mitochondrion*, **7**, 127–135.
39. Schulz, J.B., Boesch, S., Burk, K., Durr, A., Giunti, P., Mariotti, C., Pousset, F., Schols, L., Vankan, P. and Pandolfo, M. (2009) Diagnosis and treatment of Friedreich ataxia: a European perspective. *Nat. Rev. Neurol.*, **5**, 222–234.
40. Tsou, A.Y., Friedman, L.S., Wilson, R.B. and Lynch, D.R. (2009) Pharmacotherapy for Friedreich ataxia. *CNS Drugs*, **23**, 213–223.
41. Goldberg, A.V., Molik, S., Tsaousis, A.D., Neumann, K., Kuhnke, G., Delbac, F., Vivares, C.P., Hirt, R.P., Lill, R. and Embley, T.M. (2008) Localization and functionality of microsporidian iron–sulphur cluster assembly proteins. *Nature*, **452**, 624–628.
42. Mueller, J.C., Andreoli, C., Prokisch, H. and Meitinger, T. (2004) Mechanisms for multiple intracellular localization of human mitochondrial proteins. *Mitochondrion*, **3**, 315–325.
43. Karniely, S. and Pines, O. (2005) Single translation–dual destination: mechanisms of dual protein targeting in eukaryotes. *EMBO Rep.*, **6**, 420–425.
44. Regev-Rudzki, N., Yogev, O. and Pines, O. (2008) The mitochondrial targeting sequence tilts the balance between mitochondrial and cytosolic dual localization. *J. Cell. Sci.*, **121**, 2423–2431.
45. Sass, E., Blachinsky, E., Karniely, S. and Pines, O. (2001) Mitochondrial and cytosolic isoforms of yeast fumarase are derivatives of a single translation product and have identical amino termini. *J. Biol. Chem.*, **276**, 46111–46117.
46. Gruer, M.J., Artymiuk, P.J. and Guest, J.R. (1997) The aconitase family: three structural variations on a common theme. *Trends Biochem. Sci.*, **22**, 3–6.
47. Puccio, H., Simon, D., Cossée, M., Criqui-Filipe, P., Tiziano, F., Melki, J., Hindelang, C., Matyas, R., Rustin, P. and Koenig, M. (2001) Mouse models for Friedreich ataxia exhibit cardiomyopathy, sensory nerve defect and Fe–S enzyme deficiency followed by intramitochondrial iron deposits. *Nat. Genet.*, **27**, 181–186.
48. Seznec, H., Simon, D., Bouton, C., Reutenauer, L., Hertzog, A., Golik, P., Procaccio, V., Patel, M., Drapier, J.C., Koenig, M. *et al.* (2005) Friedreich ataxia: the oxidative stress paradox. *Hum. Mol. Genet.*, **14**, 463–474.
49. Anderson, P.R., Kirby, K., Hilliker, A.J. and Phillips, J.P. (2005) RNAi-mediated suppression of the mitochondrial iron chaperone, frataxin, in Drosophila. *Hum. Mol. Genet.*, **14**, 3397–3405.
50. Cairo, G., Recalcati, S., Pietrangelo, A. and Minotti, G. (2002) The iron regulatory proteins: targets and modulators of free radical reactions and oxidative damage. *Free Radic. Biol. Med.*, **32**, 1237–1243.
51. Brazzolotto, X., Gaillard, J., Pantopoulos, K., Hentze, M.W. and Moulis, J.M. (1999) Human cytoplasmic aconitase (Iron regulatory protein 1) is converted into its [3Fe–4S] form by hydrogen peroxide in vitro but is not activated for iron-responsive element binding. *J. Biol. Chem.*, **274**, 21625–21630.
52. Brown, N.M., Kennedy, M.C., Antholine, W.E., Eisenstein, R.S. and Walden, W.E. (2002) Detection of a [3Fe–4S] cluster intermediate of cytosolic aconitase in yeast expressing iron regulatory protein 1. Insights into the mechanism of Fe–S cluster cycling. *J. Biol. Chem.*, **277**, 7246–7254.
53. Soum, E., Brazzolotto, X., Goussias, C., Bouton, C., Moulis, J.M., Mattioli, T.A. and Drapier, J.C. (2003) Peroxynitrite and nitric oxide differently target the iron–sulfur cluster and amino acid residues of human iron regulatory protein 1. *Biochemistry*, **42**, 7648–7654.
54. Pantopoulos, K. and Hentze, M.W. (1998) Activation of iron regulatory protein-1 by oxidative stress *in vitro*. *Proc. Natl. Acad. Sci. USA*, **95**, 10559–10563.
55. Deck, K.M., Vasanthakumar, A., Anderson, S.A., Goforth, J.B., Kennedy, M.C., Antholine, W.E. and Eisenstein, R.S. (2009) Evidence that phosphorylation of iron regulatory protein 1 at Serine 138 destabilizes the [4Fe–4S] cluster in cytosolic aconitase by enhancing 4Fe–3Fe cycling. *J. Biol. Chem.*, **284**, 12701–12709.